Construction and Building Materials 362 (2023) 129758

Contents lists available at ScienceDirect

Construction and Building Materials

journal homepage: www.elsevier.com/locate/conbuildmat

Biocementation of coral sand under seawater environment and an improved three-stage biogrouting approach

Rui Xiao [a,c], Beiye Liang [b], Feng Wu [b], Linchong Huang [b], Zhengshou Lai [a,*]

[a] School of Intelligent Systems Engineering, Shenzhen Campus of Sun Yat-sen University, Shenzhen 518107, China
[b] School of Aeronautics and Astronautics Engineering, Shenzhen Campus of Sun Yat-sen University, Shenzhen 518107, China
[c] Center for Synthetic Biochemistry, Institute of Synthetic Biology, Shenzhen Institutes of Advanced Technologies, Shenzhen, Guangdong 518055, China

ARTICLE INFO

Keywords:
Biocementation
Coral sand
Seawater environment
Sporosarcina pasteurii
Ureolysis activity inhibition

ABSTRACT

The *Sporosarcina pasteurii (S. pasteurii)-DSM 33* was acclimated to grow and secrete urease under different salinity level conditions via direct evolution method, and ultimately the new acclimated species, *S. pasteurii-DSM 33-ASW100*, was of higher cell growth rate and ureolysis activity under seawater environment. Meanwhile, this study further revealed a fact that high concentration of calcium chloride (>0.25 mol/L) would inhibit the existing urease activity but hardly affect the urease secretion function of *S. pasteurii-DSM 33-ASW100*. The rising of urea concentration would not mitigate the inhibitory effect of calcium chloride on urease activity; by contrast, it could stimulate *S. pasteurii-DSM 33-ASW100* to secrete more urease, ultimately conducting the microbially induced carbonate precipitation (MICP) reaction under a higher pH level (~8.0). In the seawater environment, the optimal coral sand particle size for MICP reaction was about 0.5–1.0 mm. Moreover, the new designed three-stage biogrouting method significantly mitigate the issue of non-uniform distribution of cells and crystals in the column, thereby greatly increasing the unconfined compressive strength of MICP-treated coral sand column (>9.0 MPa) with a relatively high $CaCO_3$ content (~32 % by weight) as well as calcium ion utilization rate (~85 %). Results also indicated that excessive input of $CaCl_2$ (>0.5 mol/L) may result in less uniformity of crystallization and thus lead to a relative lower unconfined compressive strength (~4.0 MPa). Excessive addition of urea (>1.0 mol/L) may lead to partial clogging issues due to too fast reaction of MICP, consequently column strength dropping down to around 2.0 MPa.

1. Introduction

Coral sand is a type of marine sediment primarily derived from marine organisms. It is widely distributed in and also the primary geo-materials of the islands and reefs in low-latitude tropical oceans such as the South China Sea, Red Sea, the Persian Gulf, Hawaiian Islands and coastlines of Australia, India and Saudi Arabia [1]; and it has the potential to be used as a raw material for coastal shoreline restoration, construction of coastal defense system or even marine reclamation [2]. The major composition of coral sand is calcium carbonate ($CaCO_3$) which is of a certain stiffness and in company with special porous structures. Conventional cementation techniques usually involve the usage of cement, which is costly due to the need of long-distance transportation and may also have potential impacts on the eco-environments of the ocean. As an emerging eco-friendly alternative, microbially induced carbonate precipitation (MICP) [3–6] uses microorganisms to precipitate $CaCO_3$ as a binding agent for manufacturing construction materials. Using coral sand as the raw material in MICP treatment for costal engineering is a cost-effective option.

In MICP, the cement formed via microorganism activities is called biocement, which refers to $CaCO_3$ deposit that is formed due to the rising of pH in the system rich of calcium ions. The primary role of microorganism is to create an alkaline environment by hydrolysis urea for ammonia production, and finally the ammonia reacts with water to form ammonium and hydroxide. Meanwhile, once the carbon dioxide (CO_2) enters the water system, it will be primarily maintained in a form of carbonate due to the alkaline condition created by bacteria ureolytic activity. Ultimately, the $CaCO_3$ will be formed once the Ca^{2+} appears in the system [7]. Considering the various physiological activities, microorganisms that are capable of inducing the carbonate precipitation can be categorized into three main groups: (1) photosynthetic microorganism such as cyanobacteria and microalgae [8–10], (2) sulphate

* Corresponding author.
E-mail address: laizhengsh@mail.sysu.edu.cn (Z. Lai).

https://doi.org/10.1016/j.conbuildmat.2022.129758
Received 2 August 2022; Received in revised form 30 October 2022; Accepted 11 November 2022
Available online 23 November 2022
0950-0618/© 2022 Elsevier Ltd. All rights reserved.

reducing bacteria [11], and (3) urea utilized microorganism such as *Sporosarcina pasteurii (S. pasteurii)* [12–16] and *Bacillus* bacteria [17–21]. Among these microorganisms, urea utilized microorganism is the most popular group for MICP application due to fast reaction speed and high tolerance to hostile environment.

For the past several decades, most of the MICP studies mainly focus on pursuing high geomaterial mechanical properties (like soil strength, stiffness and permeability) and fast calcium carbonate precipitation rate and urease activity by optimizing factors, including the concentration of bacteria [22,23], temperature [24], pH [25,26], composition and concentration of cementation solution (i.e., Ca^{2+}) [27,28], grouting strategies [29,30] and soil properties (e.g., size and shape) [31], while under the fresh water environment. Few of the studies emphasizes on more complicated water system (such as seawater) or tests the MICP process under seawater environment [32]. To develop the biocementation technique of coral sand under seawater environment, the MICP microorganism's growth and ureolytic activity under high salinity condition merit further study.

Another aspect is that, to pursue higher strength, researchers have been preferring to use high calcium chloride loading rate (such as 0.5, 1.0 and 2.0 mol/L etc.) despite of the potential inhibition. Many previous studies show the high strength column often came from the high calcium ion lading rate cases (0.5, 1.0 and 2.0 mol/L etc.) [33–35]. However, there are also researches reporting that the overdose of calcium chlorides can lead to the inhibition of MICP process, especially when calcium chloride daily loading rate was over 28 ~ 55 g/L [17,27,36]. Therefore, it is necessary to further explore the potential calcium inhibition mechanism in MICP treatment. Besides the nutrients loading rate, the biocement distribution uniformity can be another problem since it will influence the overall stiffness of the bioconcrete column, especially for large on-field tests [33].

The objectives of this study come in threefold. The first is to evaluate the growth and ureolytic activities of MICP bacteria, *S. pasteurii*, under marine environment. The second is to explore the potential inhibition mechanism behind high calcium ion loading rate and its potential solution. The last is to develop a new biogrouting method for MICP treatment of coral sand to avoid partial biocement clogging and improve bacterial migration in the column, thus, to facilitate the biocementation of coral sand for future large on-field applications.

2. Material and method

2.1. S. Pasteurii culture and coral sand

Seed culture preparation: *S. pasteurii-DSM 33* was purchased from Guangdong Microbial Culture Center (GDMCC), China. The standard broth media used for seed culture preparation, containing casein peptone (15 g/L), soy peptone (5 g/L), NaCl (5 g/L) and urea (20 g/L) with pH at 7.3. Seed culture was incubated under 30 °C with a rotation speed at 150 rpm for 18 h.

Coral sand: large sand grains would require great large amount of $CaCO_3$ to establish strong bonds between the grains, whereas small sand grains may result in clogging issues. Thus, there is a necessity to optimize the grain size for highest possible UCS [37,38]. In this study, coral sand was derived from Hainan Island in South China Sea and was crushed manually by using a mortar and pestle. Crushed coral sand was sieved into different size: 0.25–0.5, 0.5–1.0, 1.0–2.0 and 2.0–3.0 mm for further study.

High salinity media preparation: the present lab-scale study aimed to evaluate cell growth under high salinity condition and MICP performance under seawater condition. Thus, artificial seawater (ASW) was used as it is reproduceable with determined concentrations of chemical components [39–42]. The salinity was defined as 100 % of ASW which containing NaCl (30.0 g/L), KCl (0.7 g/L), $MgCl_2{\cdot}6H_2O$ (10.8 g/L), $MgSO_4{\cdot}7H_2O$ (5.4 g/L) and $CaCl_2{\cdot}2H_2O$ (1.0 g/L). For preparing 1 L of 100 % of ASW, 30 g of NaCl, 0.7 g of KCl, 10.8 g of $MgCl_2{\cdot}6H_2O$, 5.4 g of $MgSO_4{\cdot}7H_2O$ and 1.0 g of $CaCl_2{\cdot}2H_2O$ are added into a 1-L beaker with 800 mL of deionized (DI) water, followed by adding 15 g of casein peptone as well as 5 g of soy peptone, ultimately extra DI water was filled to make the final volume to 950 mL. The pH of the mixture is adjusted to 7.3 by using HCl and NaOH. Next, the media containing casein peptone, soy peptone and salts are sterilized by a 15-minute autoclaving process before culture inoculation, whereas the urea stock solution (200 g/L) which was sterilized via a 0.2 μm filter. After the autoclaving process, the 950 mL mixture was allowed to cool down and an extra 50 mL of urea stock solution (400 g/L) was added to make the final urea concentration into 20 g/L.

High salinity acclimated culture: *S. pasteurii-DSM 33* was enriched from the standard media after one batch. For the next four batches culture transfer, the salinity in the media was gradually increased from 25 % to 50 %, 50 % to 75 %, 75 % to 100 % and finally maintained in the 100 % ASW media for further study. During the culture transfer process, the other nutrients were kept the same as standard media. The acclimated culture was named as *S. pasteurii-DSM 33-ASW100* in this study.

2.2. Influence of salinity level on cell growth and urease activity

S. pasteurii-DSM 33 was tested under different ASW strength levels (0 %, 25 %, 50 %, 75 % and 100 %). Meanwhile, the high salinity acclimated culture (*S. pasteurii-DSM 33-ASW100*) was also tested as a comparison. The other operating conditions were fixed the same as seed culture growth condition. For every-three hours cell density and urease activity were tested.

2.3. Influence of $CaCl_2$/urea molar ratio on the pH variation

To study the effect of $CaCl_2$ and urea on bacteria metabolic activities in the MICP process, the pH variation test was conducted in the beaker under different $CaCl_2$ and urea concentrations and combinations (Table 1). The traditional cell density and urease activity measurement methods are not suitable for this experiment since the presence of calcium precipitation will influence the absorbance from ultraviolet–visible (UV-vis) spectroscopy [29]. Therefore, the MICP activity was estimated based on the pH variation, since the hydrolysis of urea in MICP process can lead to the increase of pH value. The high salinity acclimated culture was used for this test, and we assumed that urease secreted from *S. pasteurii-DSM 33* is extracellular enzyme. The 12-hour cultivated broth was collected and prepared under different treatments: the entire broth (cell + urease) was directly tested under different $CaCl_2$ and urea concentration levels (mole/L, abbreviated as

Table 1
Experiment design of different urea and $CaCl_2$ combinations and treatments.

Urea (M)	$CaCl_2$ (M)	Treatments		
		cell + urease	cell only	urease only
0.5	0.0	√	√	√
0.5	0.25	√	√	√
0.5	0.5	√	√	√
0.5	1.0	√	√	√
0.25	0.25	√		
0.5	0.25	√		
1.0	0.25	√		
0.5	0.5	√	√	√
1.0	0.5	√		
2.0	0.5	√		
3.0	0.5	√		
4.0	0.5	√	√	√
0.5	1.0	√	√	√
1.0	1.0	√		
2.0	1.0	√		
3.0	1.0	√		
4.0	1.0	√		
6.0	1.0	√		
8.0	1.0	√	√	√

M); cell and urease in the broth were separated via a 0.2 μm filter, cell maintained on the filter (cell only), and the filtrate (urease only) were collected separately for further test. 50 mL of different treatment culture samples were firstly placed in a beaker and the pH value was adjusted to 7.0, followed by mixing with different $CaCl_2$ and urea levels combinations under room temperature. pH values were recorded every 5 min for the first 30 min, 30 min from 0.5 to 2 h and 60 min for the rest of 5 h.

2.4. Fabrication of biocemented columns and the two-stage biogrouting approach

Biocement column preparation: for each 50-mL centrifuge tube column, the bottom of the column was inserted with one piece of scrub sponge as filter and a cap was semi-screwed on it to prevent sand dropping down. A certain amount of coral sand was filled into the column (with inner diameter 2.5 cm) up to a height of 5.0 cm. A piece of wax weighing paper was placed between tube wall and sand to improve tube and biocement column separation. One piece of scouring pad was paved on the top of the sand column to prevent cell partially accumulation and clogging (Fig. 1a).

Two-stage biogrouting method: the experiment was started by connecting the pump with biogrout solution, and thus letting the biogrout solution pumping into the column from the top and drain out from the bottom (Fig. 1b). The pumping flow rate was controlled under 3 mL/min. The first step (1st stage) was cell recycling. To facilitate the bacteria to enter the column, 25 mL of the high salinity acclimated cell broth after 12 h incubation was diluted by DI water, which lead to the optical density (OD_{600}) at around 1.0–1.2 under 600 nm and mixed with sand for 1–2 h. In step 2 (2nd stage), 50 mL of 100 % ASW strength media mixed with a certain amount of $CaCl_2$ and urea was recirculated in the column for 21–22 h. No pH adjustment was needed for all these steps. The solution in each step was agitated by a stir bar (~200 rpm) to supply sufficient air for cell survival in the column [39]. The circulation system was paused after 4–10 recycling days when the pumping flow rate was decreased to 1 mL/min and solution can hardly be drained out from the bottom of column. The residual solution in the column was dumped. After that, the whole tube was put into oven (~60 °C) for 30 min. Then, the sand column was pushed out of the tube and was kept drying under 60 °C for another 48 h. The completely dried column sample was placed at room temperature for unconfined compression strength (UCS) test and Ca^{2+} conversion efficiency measurements.

2.5. Influence of particle size on the strength of coral sand columns

In the particle size tests, four different size ranges (0.25–0.5, 0.5–1.0, 1.0–2.0 and 2.0–3.0 mm) were tested with $CaCl_2$ and urea daily loading rate at 0.5 M and 1.0 M, respectively. The two-stage grouting procedures in section 2.4 were implemented for this section. The UCS, grouting pH and Ca^{2+} converting efficiency were measured for all the column samples.

2.6. The three-stage biogrouting method

To facilitate *S. pasteurii-DSM 33* cells and $CaCO_3$ crystals to distribute and form in the large size column sample uniformly as well as to prevent partially clogging under high urea loading rate, a modified three stage grouting method was developed. The first step (1st stage, cell circulation) was still cell recycling. 25 mL of the high salinity acclimated cell broth after 12 h incubation was diluted by DI water (OD_{600} = 0.4–0.8) and mixed with sand for 1–2 h. The cell broth was added stepwise in three steps (30–40 % of total cell broth per step for every 30 min). The OD_{600} values can raise from 0.4 to 0.8 after three batch additions. Due to the water surface tension, the alkaline solution (cell broth) from stage 1 cannot be completely drained out of the column by gravity. Thus, to avoid the immediate reaction between OH^- (from alkaline solution) and $CaCl_2$ from previous step 2 (section 2.4), the alkaline solution from broth should be washed out by clean water to prevent partially clogging at the top layer of the column. Hence, in new step 2 (2nd stage, water wash), 50 mL of DI water was drained down (3 mL/min) to wash the alkaline solution residual out of the column then followed by step 3 (3rd stage, biocement solution circulation), 50 mL of 100 % ASW strength media mixed with a certain amount of $CaCl_2$ and urea was recirculated in the column for 20–21 h (Fig. 2).

As a consideration of time consuming of the column drying procedure of lab-scale MICP, this study selected to dry the columns under 60 °C, which is a common and efficient approach to remove moisture in the column and thus to preciously determine the calcium utilization and $CaCO_3$ content of each column [40,41]. Some guidelines for future large-scale field tests based on the present lab-scale three-stage biogrouting method are provided as below: 1) clean water is not a requisite, whereas water from river or lake and seawater are all suitable washing reagents for field tests; 2) the 60 °C drying step is not necessary in field tests; instead, the MICP sample can be naturally dried or even tested without drying, as the MICP process could proceed under the water or seawater environment; 3) the pumping system in this study was primary designed

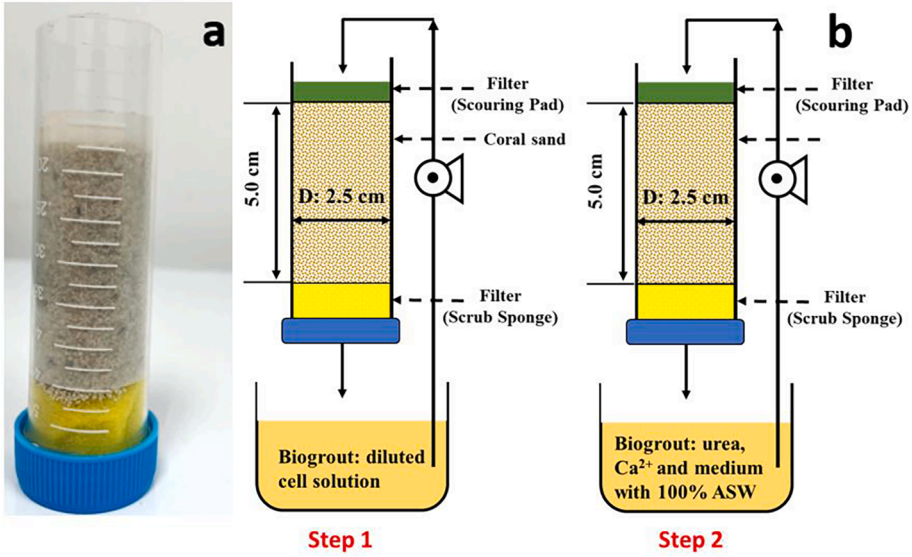

Fig. 1. (a) Biocement column setup and (b) procedures of two-stage biogrouting method.

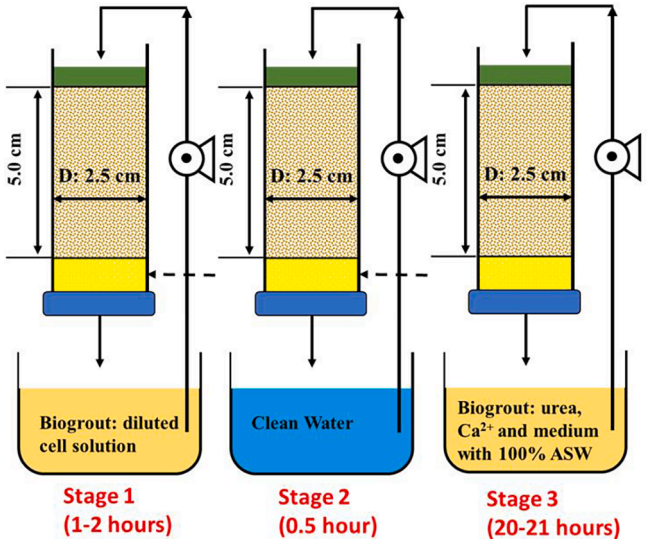

Fig. 2. Procedures of three-stage biogrouting method.

for lab-scale tests. For pumping in field tests, engineers can insert multiple pipes with pours on it into the soils or sands to enhance crystallization homogeneity; 4) cell broth and water wash reagent would be better to be pumped from the bottom of the pipes to make use of the pressure gradient at deep water environment.

2.7. Influence of urea/$CaCl_2$ molar ratio on the strength of coral sand columns

To investigate the influence of $CaCl_2$ loading rate on biocement column strength, sand particle size at 0.5–10 mm with different daily $CaCl_2$ loading levels (0.25, 0.5 and1.0 M) were tested while the urea/$CaCl_2$ molar ratio were kept at 1:1. On the other hand, to investigate the influence of urea loading rate on biocement column strength, the urea daily loading rates were varied from 0.5 to 4.0 M under a constant $CaCl_2$ loading rate (0.5 M). The three-stage biogrouting procedures in section 2.6 were implemented for this section. The UCS, biogrouting pH and Ca^{2+} converting efficiency were measured for all the column samples.

2.8. Characterization and testing methods

Cell growth determination: the cell growth was measured by using UV-vis spectrophotometer under the wavelength at 600 nm [42]. The standard cell cultivation media was used as the background control and OD_{600} value was used to represent the cell density in all the cell growth tests.

Urease activity measurement: the urease activity was determined following the Whiffin's approach [29]. 1 mL of bacterial suspension was first mixed with 9 mL of urea stock solution (66 g/L), after which the mixture is further diluted by 10 times with 90 mL of DI water. The urease activity was calculated based on the conductivity variation within 5 min.

Ca^{2+} utilization efficiency and $CaCO_3$ content: the calcite crystal content in the biocement coral sand column cannot be determined by directly measuring $CaCO_3$ content since the major composition of coral sand is also $CaCO_3$. Therefore, the $CaCO_3$ content was estimated based on weight difference between the column weight before and after circulation (Eq. (1)). Meanwhile, the amount of cell that enters the column should also be subtracted. Moreover, in term of the economic efficiency, the Ca^{2+} conversion efficiency ($CaCl_2$ to $CaCO_3$) is also considered and is calculated as

$$CaCO_3\ content\ (\%) = \frac{m_{after} - m_{before} - n\,m_{cell}}{m_{after} - n\,m_{cell}} \times 100\% \quad (1)$$

$$Utilization\ efficiency(\%) = \frac{(m_{after} - m_{before} - n\,m_{cell})/MW_{CaCO3}}{QVn/MW_{CaCl2}} \times 100\% \quad (2)$$

where m_{before} is the column weight before circulation (g); m_{after} is the column weight after circulation (g); m_{cell} is the weight of cell enters column each cycle (g), based on the change of diluted cell broth OD_{600} values before and after circulation (data not shown), we assume 90 % of cell maintained in the column after cell circulation. For a 25 mL broth, the cell dry weight was 0.12 g; n is the number of circulation cycles; Q is the $CaCl_2$ daily loading rate (g/L); V is the volume of circulation solution in stage 2 (mL); MW_{CaCO3} and MW_{CaCl2} are the molecular weight of calcium carbonate (g/mole) and calcium chloride (g/mole), respectively.

Unconfined compression strength (UCS): the unconfined compression test was conducted using a universal testing machine (Fig. 3) following the ASTM C39 standard. The specimen is placed between two compression plates and is loaded by pushing the top plate downwards. In this work, the compressive loading rate is kept constant at 1.0 mm/min, which is consistent with Cheng et al. [43] for testing biocemented columns. The force and displacements of the top plate are recorded during the test, based on which the stress and strain are computed. Specifically, the stress is calculated as the loading force divided by the cross-sectional area of the specimen, whereas the strain is calculated as the displacement of the top compression plate divided by the initial height of the specimen. The UCS is taken as the maximum stress that the specimen could sustain.

Scanning electron microscopy (SEM): the small piece of biocemented sand was taken from the crushed column sample after UCS test. The small piece biocemented sand was coated with platinum and scanned under a relative low voltage beam (3.0 kV). The sample surface was amplified to different resolution levels (5–100 μm) to record the clearest crystal structure.

3. Results and discussion

3.1. Cell growth and urease active under different salinity levels

To test the cell resistant ability to seawater environment, seed culture was transferred into different levels of salinity (0, 25, 50, 75 and 100 % of ASW) media for cell growth and urease activity test. Meanwhile, the performance of growth and urease activity from acclimated culture (*S. pasteurii-DSM 33-ASW100*) was used as a comparison.

Results shown that for cell grown under 0 % ASW, the cells entered the growth phase after 3 h incubation; while for the other salinity levels (25–100 % ASW) conditions, the cells were observed to exhibit a similar growth trend but with lower growth rates. For salinity levels at 25 and 50 %, the cell growth had a very close increasing trend to the 0 % ASW condition but with the slightly lower OD values before 12th hour. However, for salinity levels at 75 and 100 %, the OD_{600} value had a relative lower increasing trend from 6th to12^{th} and 15th hour, respectively (Fig. 4a). The potential reason behind this observation was that the cells need time to change the cell membrane permeability by adjusting osmotic pressure due to the sudden change of salinity from 0 % to 75 % and 100 % ASW [44]. The higher variation of salinity, the longer time would be needed to reach the highest growth rate. Ultimately, after 12–15 h incubation, cultures with all the salinity conditions (0–100 % ASW) had completely reached the exponential growth phase and entered stationary phase in 21 h.

The maximum cell density (indicated by the maximum OD_{600} of 6.0) was obtained after 24 h of incubation (Fig. 4a). It indicated that *S. pasteurii-DSM 33* was capable of growing in the seawater environment and had certain resistance to high salinity strength. Similar results were also reported by Fu et al.[45], where the *S. pasteurii* was shown to be capable of growing under seawater condition without significant inhibition. On the other hand, the growth performance of acclimated culture

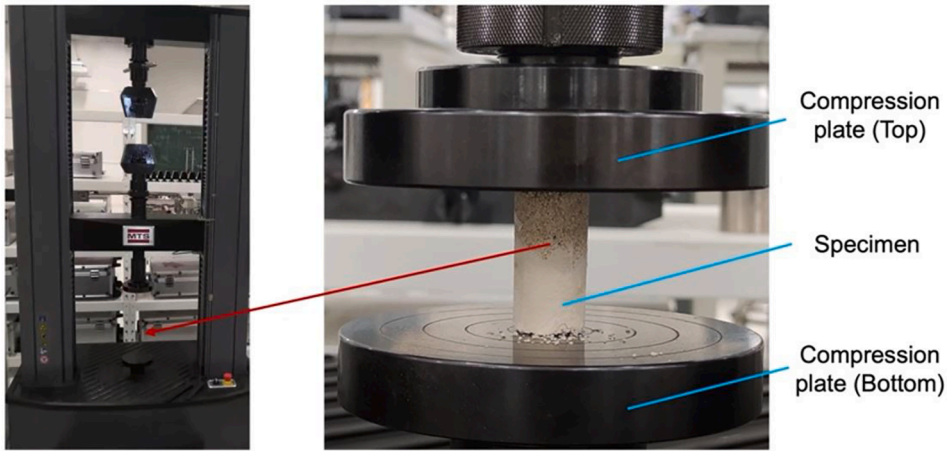

Fig. 3. Universal testing machine and the setup for the UCS test of biocemented coral sand column.

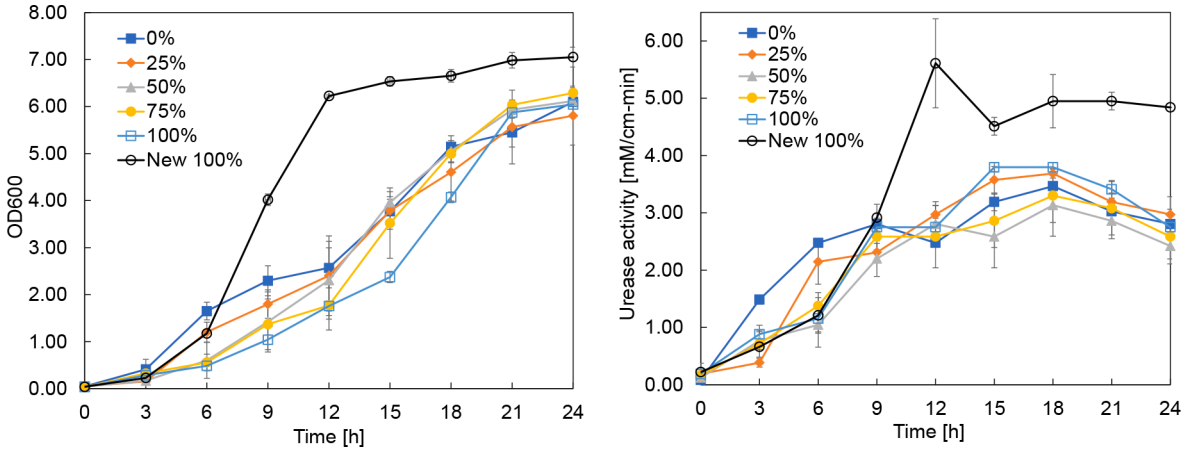

Fig. 4. Cell growth (a) and urease activity (b) under different salinity levels within 24 h incubation (New 100% represents acclimated culture, *S. pasteurii-DSM 33-ASW100*).

(New 100 %ASW) from Fig. 4a reflected that *S. pasteurii-DSM 33-ASW100* completely entered exponential growth phase in 6th hour and reached to stationary phase after 12 h incubation with a final OD_{600} at 7.0. Compared with standard culture, the growth rate from *S. pasteurii*-DSM 33-ASW100 had been nearly doubled and the maximum cell density was 14 % higher than the standard seed culture. This result reflected that long-term cultivation under high salinity condition (100 %ASW) improved the cell growth rate and maximum cell density of *S. pasteurii*.

Urease, as one of the extracellular enzymes from *S. pasteurii-DSM 33*, functions as facilitating the hydrolyzation of urea, providing alkaline condition for calcite crystal formation. The urease activity under different growth phase is critical to cell circulation stage in the grouting process. Proper cell cultivation time with the relative high cell density and urease activity for cell circulation stage need to be selected. The urease activity from Fig. 4b shown that the temporal urease activities had similar trend to the cell growth (Fig. 4a), which indicated that the production of urease from *S. pasteurii* is growth-associated. The slight decrease of urase activity after 21 h may be due to the lower urea concentration in the media since higher substrate concentration comes with higher enzyme activity. It is worth noting that the maximum urease activity (5.5 mM/cm-min) was achieved at 12th hour from *S. pasteurii-DSM 33-ASW100*, which was corresponding to a relative high cell density (OD_{600} = 6.2) at the beginning of stationary phase. This finding gives a clue that higher urease activity can be obtained under high salinity pressure. High salinity inducing fermentation could be a potential effective approach to obtain a *S. pasteurii* culture with high cell density and urease activity. Hence, *S. pasteurii-DSM 33-ASW100* with 12-hour incubation time was selected for the rest of the studies.

3.2. *pH variation with time under different $CaCl_2$/urea concentrations and molar ratios*

3.2.1. *Potential MICP inhibition mechanism under different $CaCl_2$ level*

The results of pH for the cases of different $CaCl_2$/urea levels and molar ratios are plotted in Fig. 5. At the very beginning, the pH was manually adjusted to 7.0 for all the batches to facilitate the investigation of $CaCl_2$/urea concentrations and molar ratios effects. After adding $CaCl_2$/urea, the pH was dropping down rapidly since $CaCl_2$ is a Lewis acid. It forms calcium hydroxide and liberates the hydrogen ions, causing the pH to become lower at the beginning of each batch (Fig. 5a–d). After that, pH increases gradually due to the MICP process. Results from Fig. 5a indicate that the pH values for the case of $CaCl_2$ concertation over 0.5 M were below 7.0, while the pH for the case of $CaCl_2$ at 0.25 M gradually increased to 8.0 after 1.5 h. Comparing with the control batch (0.0 M $CaCl_2$), the results indicate that MICP process was partially activated when $CaCl_2$ concentration was below 0.25 M, while it was inhibited when $CaCl_2$ was over 0.5 M.

In the next step, different urea concentration levels were tested under different $CaCl_2$ loading rate (0.25, 0.5 and 1.0 M). It was found that pH under different urea loading rates (0.25–1.0 M) increased over 8.0 within 6-hour incubation when the $CaCl_2$ loading rate was kept at 0.25 M (Fig. 5b). The only difference was that the pH increasing rate was

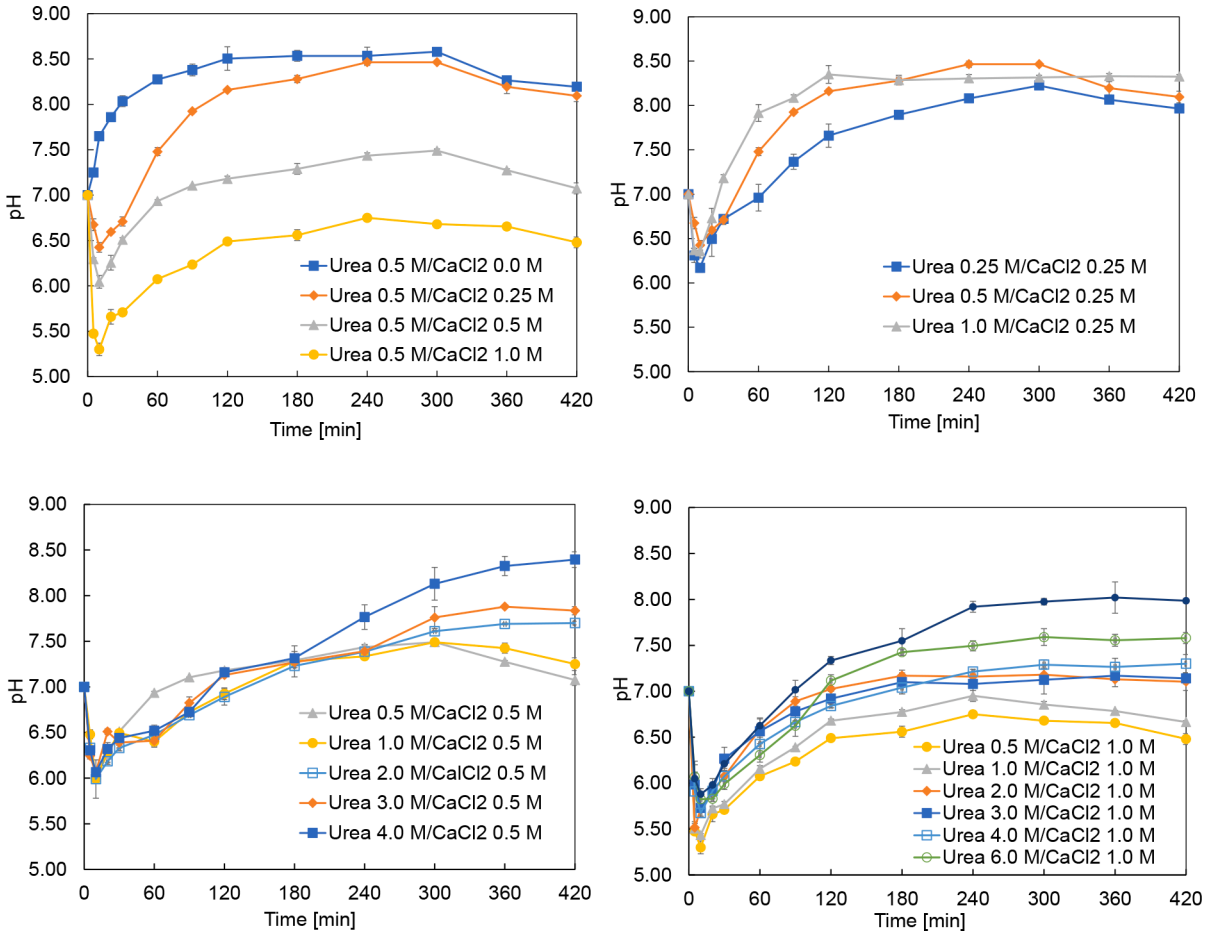

Fig. 5. Evolution of pH with time under different Urea/$CaCl_2$ concentrations: (a) cell + urease treatment with fixed concentration (0.5 M) of urea and varying concentration of $CaCl_2$, (b) cell + urease treatment with varying concentration of urea and fixed concentration (0.25 M) of $CaCl_2$, (c) cell + urease treatment with varying concentration of urea and fixed concentration (0.5 M) of $CaCl_2$, and (d) cell + urease treatment with varying concentration of urea and fixed concentration (1.0 M) of $CaCl_2$.

higher when urea concentration was over 0.5 M. The reason behind this observation is that higher substrate concentration can lead to a higher hydrolysis rate, and thus, higher urea concentration can promote higher urease activity, eventually leading to higher pH increasing rate.

In addition to the urea concentration under low $CaCl_2$ loading rate, the different urea loading rates under high $CaCl_2$ levels (0.5 and 1.0 M) were also investigated. It was surprisingly found that with the increase of urea loading rate, the pH raised up to 8.0 after 4 h incubation for both two $CaCl_2$ levels (0.5 and 1.0 M) when the molar ratio of urea/$CaCl_2$ was increased to 8:1 (Fig. 5c and d). This finding suggested that high urea loading rate can somehow overcome the inhibition from high $CaCl_2$ concentration. The stress caused by high $CaCl_2$ concentration levels appeared to inhibit the bacteria ureolytic activity and urease hydrolysis function. The similar inhibition mechanism was also put forward by Svane et al. [46]. On the other hand, the high urea loading can mitigate the inhibition effects. However, the exact mechanisms behind the findings about high urea concentration promoting the rising of pH require further investigation.

3.2.2. *Potential urease inhibition style under high $CaCl_2$ level*

Motivated by the above interesting observations and aiming at revealing the underlying mechanism of MICP inhibition due to high $CaCl_2$, the cells were further separated by using the 0.2 μm membrane after 12 h incubation. The cell cake maintained on the membrane was again mixed with fresh 100 % ASW media (cell only) while the filtrate with urease included was directly used as the urease only treatment. Both treatments were tested under different $CaCl_2$ levels (0.0, 0.25, 0.5 and 1.0 M) with a fixed level of urea concentration (0.5 M). Results from cell only treatments showed that pH increased to 8.5 after 15 min if no $CaCl_2$ was added; while it took 3 h for the pH to increase to 8.0 when $CaCl_2$ is 0.25 M. The pH values kept below 7.5 when $CaCl_2$ level goes to 0.5 M (Fig. 6a). In contrast to cell only treatment, the urea only treatment results show that all the pH values maintained below 7.5 for all the $CaCl_2$ levels (0.25–1.0 M) except the control batch($CaCl_2$ at 0.0 M) (Fig. 6b), indicating that enzyme activity can be strongly inhibited even under a relative low $CaCl_2$ concentration level (0.25 M), while ureolytic activity from *S. pasteurii-DSM 33-ASW100* can overcome this inhibition but will be strongly inhibited under high $CaCl_2$ levels (0.5–1.0 M). These findings could be because that the urease activity was inhibited by $CaCl_2$ by binding with the urease active sites or the binding of the inhibitor ($CaCl_2$) to the allosteric site causes a conformational change to the enzyme's active site, ultimately ceasing the hydrolysis reaction. In the cell only treatments, enzyme inhibition effect was still there, however, the cell can utilize the nutrients and urea to keep continuously producing new urease. Therefore, we assume that at the beginning of MICP, all the $CaCl_2$ molecules will bind with previous urease activity sites and the ureolysis rate could not raise back (pH raised up) unless more new activity sites are provided from cells by secreting more urease. Similar results was reported in Zhao et al. [47] that cells can keep growing during the MICP process and continuously producing new urease, which improves the urease activity.

To address the potential enzyme inhibition style, two different urea concentration levels were further studied under two different high $CaCl_2$ levels (0.5 and 1.0 M). It was noticed that for the urease only treatments,

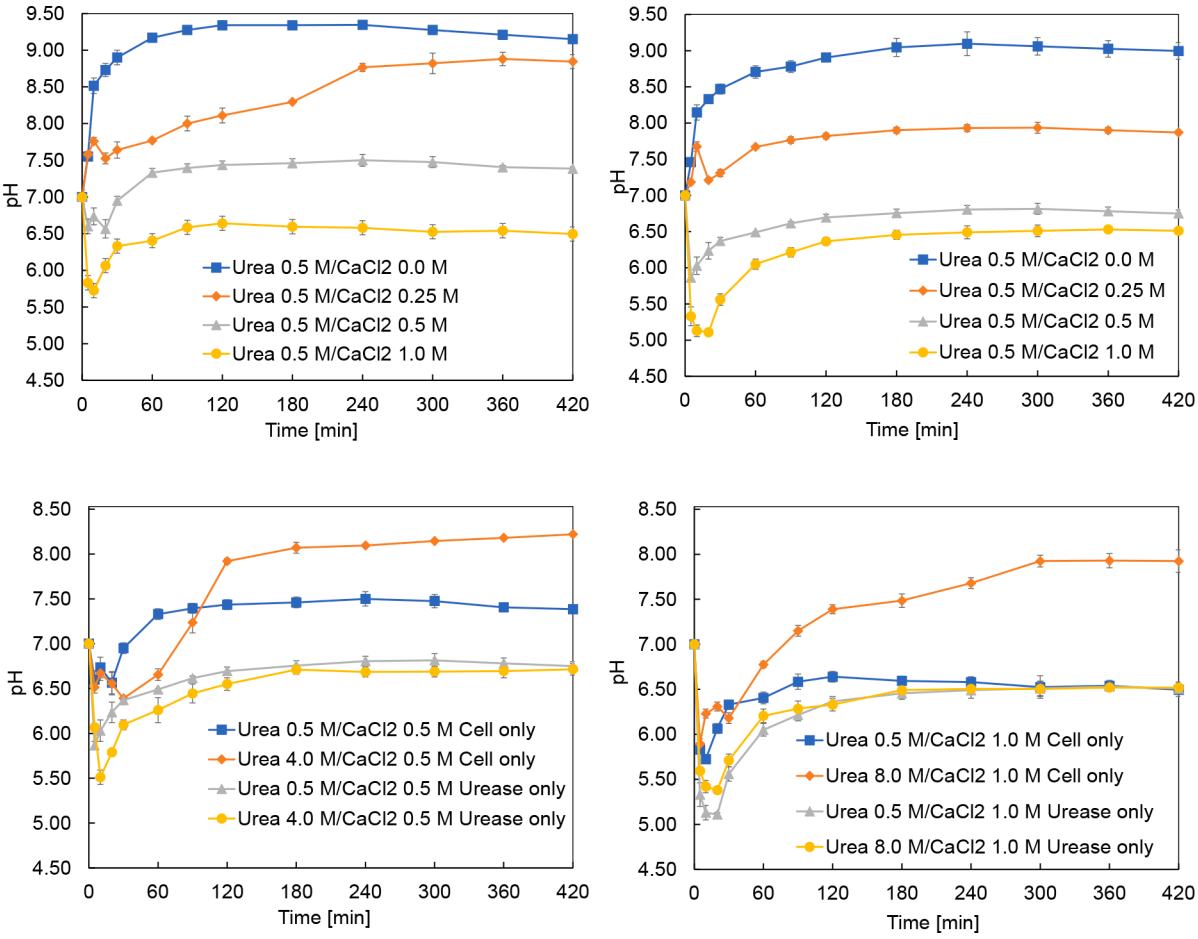

Fig. 6. Evolution of pH with time under different Urea/$CaCl_2$ concentration levels and treatments: (a) cell only treatments with urea under 0.5 M, (b) urease only treatments with urea under 0.5 M, (c) cell only and urease only treatments with $CaCl_2$ under 0.5 M, and (d) cell only and urease only treatments with $CaCl_2$ under 1.0 M.

none of the pH could raise above 6.5 within 7 h even after the urea/$CaCl_2$ ratio was increased to 8:1 for both different high $CaCl_2$ levels (0.5 and 1.0 M) (Fig. 6c and d). This phenomenon indicated that ureolysis activity cannot be recovered by adding extra more substrate (urea), thus the potential inhibition type was probably the noncompetitive inhibition. The enzyme inhibition hypothesis was also put forward in other studies [46,48,49], however, no specific inhibition style was further clarified.

As to cell only treatments, higher urea/$CaCl_2$ ratio (8:1) can promote pH to rise, especially under $CaCl_2$ of 0.5 M. The solution pH raised to 8.0 within 2 h incubation (Fig. 6c). In addition, the solution pH also gradually climbed up to 8.0 in the 5th hour when urea concentration was 8.0 M with a $CaCl_2$ loading rate at 1.0 M (Fig. 6d). This finding indicated that high urea concentration can induce bacteria producing more urease and enhance ureolysis activity for faster pH arising. Moreover, high $CaCl_2$ loading rate (0.5–1.0 M) had negative effect to the ureolytic activity from *S. pasteurii-DSM 33-ASW100* but can be overcame by adding large amount of urea. Further increasing $CaCl_2$ concentration (>1.0 M) is not recommended since the massive of $CaCl_2$ will form large size crystal, encapsulating most of the cell in it and reducing the microbial activity. Similar substrate inducing phenomenon was observed from our previous study that adding specific polysaccharides can induce the corresponding hydrolysis enzyme secretion [50]. Considering all above, the $CaCl_2$ loading rate should be kept under a moderate level (~0.5 M) as high level $CaCl_2$ loading rate may result in the MICP process conducting under a very low pH condition, which ultimately makes a negative impact on the calcite crystal morphology and column strength [26].

3.3. Effect of coral sand particle size

In general, the size of *Bacillus* and *Sporosarcina* cells is around 1–5 μm [31], thus neither too small (e.g., clay <1 μm) nor too large (e.g., coarse sand, gravel etc.) particle size is favored for high strength biocemented column. On one hand, small particle size could lead to small porosity which would have negative effect on the cell and crystal uniformity; on the other hand, cells are difficult to maintain in the large particle size column and most of the $CaCO_3$ may attach to only the surface of particles instead of the contact points between particles. Therefore, it is essential to find the proper range of particle size to approach an optimal biocementation, in terms of strength and efficiency.

With the same cell loading rate (OD = 1.0–1.2) and $CaCl_2$/urea concentration level (0.5/1.0 M), particle size under 0.5–1.0 mm

Table 2
Column properties for different coral sand particle size.

Sand particle size (mm)	0.25 ~ 0.5	0.5 ~ 1.0	1.0 ~ 2.0	2.0 ~ 3.0
UCS (MPa)	1.3 ± 0.49	2.2 ± 1.2	0.36 ± 0.2	0.39 ± 0.3
Biocement solution pH	7.1 ± 0.5	7.2 ± 0.7	7.4 ± 0.6	7.3 ± 0.4
Ca^{2+} utilization efficiency (%)	83.4 ± 2.0	79.0 ± 4.2	59.2 ± 2.4	58.4 ± 8.3
$CaCO_3$ content (%)	15.0 ± 0.4	19.8 ± 0.7	19.9 ± 0.6	28.9 ± 4.0

achieved the highest UCS, followed by the size at 0.25–0.5 mm (Table 2). For the case of smaller particle size, fewer cells could get into the column for MICP, which eventually leads to limited and less uniform calcium carbonate precipitation in the column [17,51]. Another explanation behind this phenomenon is that the extracellular polymeric substance (EPS) formed by the cells is of high viscidity, which prohibits the cells from migrating in a large cluster form, thus resulting in cells massively accumulating at the top layer of column. On the contrary, the strength of the column began to decrease when particle size was over 1.0 mm, whereas the highest $CaCO_3$ content was observed under the particle size at 2.0–3.0 mm (Table 2). This could be the reason that large particle size is always accompanied with large voids, hence needs more $CaCO_3$ to fill out the empty space, resulting in more circulation days and large amount of $CaCl_2$ input. In addition, for larger particles, due to less inter-granular contacts and larger inter-granular distance, crystals primarily attached to the surface of particles rather than the contact points, which finally weakened the stiffness of column [17]. This could also be the reason that calcium ions cannot efficiently attach to the outer surface of the cells due to large flowing space, resulting in less contacting with urease at the outer surface of the cells and finally leading to a relative lower Ca^{2+} utilization efficiency compared with other small size range (0.25–1.0 mm). In sum, considering the high UCS, relatively high Ca^{2+} utilization efficiency and $CaCO_3$ content, the particle size at 0.5–1.0 mm was selected for the rest of tests.

For practical applications, the coral sand particle size is also important to engineering practices such as coastline restoration and ground stabilization. The proper particle size can enhance engineering mechanical properties. In some reef regions in South China Sea, coral sand has been drilled, crushed, and pumped to the reef from deep ocean to improve the stabilization [52–54]. In the future, the MICP technique could be combined with the hammer vibration technique to improve the bearing capacity of the reclaimed foundation, where particle size would be an important factor for design.

3.4. Biocementation with three-stage biogrouting approach

To create a more uniform crystallization environment in the column, cell broth OD in the step 1 was decreased to 0.4–0.8 and was added via fed-batch mode. The fed-batch cell recirculation mode can let cell easily migrate to the bottom of the column under low cell broth concentration (OD = 0.4), whereas cells would stay at the middle or top of the column when cell broth concentration gradually increases to OD at 0.8. Moreover, an extra step was added between cell and media recirculation steps. The main purpose of water wash step (step 2) is to remove extra alkaline solution generated from the 12 h-cell broth and prevent fast forming of $Ca(OH)_2$ or $CaCO_3$ at the top of the column. As such, MICP process can proceed moderately without clogging the top layer of the column. According to the results of section 3.3, the molar ratio of $CaCl_2$/urea at 1:2 with particle size at 0.5–1.0 mm was selected for the tests of three-stage biogrouting method due to high USC (2.2 MPa) and calcium ion utilization efficiency (79 %).

The unconfined compressive stress-strain curves of the three-stage method treated samples were presented in Fig. 7. For comparison, the curves from two-stage treated samples with identical $CaCl_2$/urea molar ratio as well as particle size were also displayed in Fig. 7. For all the three-stage treated samples, the stress-strain curves were close and can be divided into four stages. In the first stage, due to the compaction of pores and fractures in the column, the stresses increased slowly at the beginning. In the second stage, the stresses increased almost linearly to the maximum (~9.9 MPa), accompanied with some small wave-shape bumps. In the third stage, the further increase of strain led to the larger wave-shape stress curves appear and the stresses were oscillating around a point (~8.0 MPa) which was slightly lower than maximum and maintained for a while. In the last stage, the stresses suddenly decreased when strain was further increased. Similar stress curves and maximum stress value were also observed in Fang et al. [55].

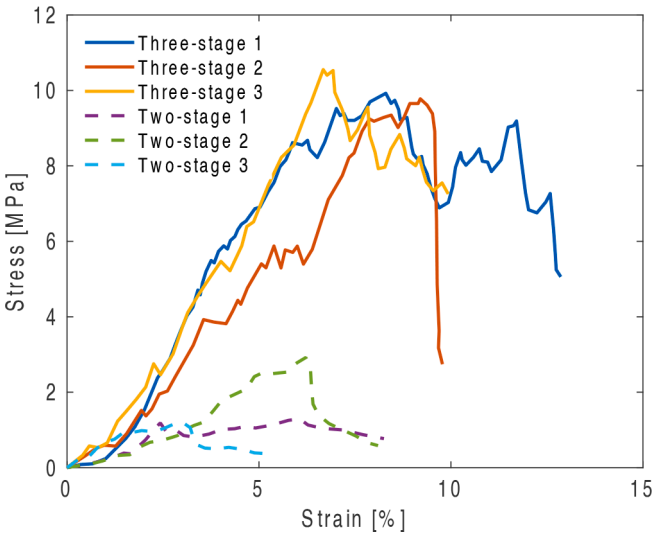

Fig. 7. UCS test results of the columns via three-stage and two stage biogrouting methods.

It is also worthwhile noting that the similar wave-shape and bumpy curves were obtained from the tensile and shear force tests of nacre structures [56]. In addition, many studies indicated that the protein-polysaccharides network structure exists in nacre and can enhance the resistance to shear and tensile [56–59]. Moreover, Zhang's group [60] directly added extra protein substance, egg white, to improve the binding of tailings particles with calcium carbonate crystals. Therefore, some extracellular EPS mainly composed of protein and polysaccharides was formed in the medium recirculation stage (third stage). The bacteria utilized the nutrients for cell growth, urease production as well as EPS accumulation. The protein-saccharides matrix provided a high adhesion to the coral sand particles, ultimately improved the stiffness of the column, and caused the bumps and oscillations in the stress-strain curves. The EPS content in the column should be further studied in the future since this organic structure is of promising resistance to shear, tensile and even compressional stresses, and has potential application in anti-seismic field.

The maximum stress values achieved from two-stage method vary from 1.0 to 3.2 MPa. The stress-strain curves present different shapes since it was very difficult to prevent accidental clogging for every daily circulation. Due to this random clogging problem, cells in the column may lack enough time, oxygen or nutrients for growth, urease formation and EPS accumulation. Hence, the stiffness of each column was relatively lower, and no bumps or oscillations were clearly observed.

Table 3 also shows that higher Ca^{2+} utilization efficiency (85.2 %) and calcium carbon content (33.4 %), which was 7 % and 40.7 % higher than two-stage biogrouting method (Table 2), could be achieved via the modified biogrouting method (i.e., three-stage). Results indicated that fed-batch cell recirculation combined with extra water wash step can generate a homogeneous distribution of cells in the column and create a uniform crystallization environment for the entire column, ultimately enhancing the strength of the sample and increasing the $CaCO_3$ converting efficiency. Meanwhile, similar to the two-stage biogrouting case, the pH of the biogrouting solution of the three-stage case could still

Table 3
Column properties via three-stage biogrouting method.

Biogrouting method	Three-stage
UCS (MPa)	9.1 ± 0.6
Biocement solution Ph	7.4 ± 0.19
Ca^{2+} utilization efficiency (%)	85.2 ± 10.4
$CaCO_3$ content (%)	33.2 ± 3.8

maintain around neutral all over the biogrouting process with slight increase (to 7.4) by the end of the last two circulation cycles. It manifested that the modification of biogrouting method would not impact much the pH of the biogrouting environment.

The microstructure of the MICP-treated samples via the three-stage grouting method are shown in Fig. 8. The coral sand surfaces were covered with $CaCO_3$ after the MICP treatment. In addition, large $CaCO_3$ crystals uniformly precipitated between particles and ultimately filled the empty spaces in the column (Fig. 8b). From the zoom in SEM photos (Fig. 8c and d), we suspected that the cells were captured by the round shape crystals since the similar round shape crystals were also observed in Ghosh et al. [61], who especially mentioned that the $CaCO_3$ crystals precipitated together with the bacteria and formed a $CaCO_3$ crystal with bacteria at its center under saline environment. In addition, those round shape crystals may be partially capsuled by the large group and some small single amorphous-shape crystals with a diameter varying from 2–10 μm (Fig. 8c and d), which are similar to the amorphous-shape crystals observed under marine environment in Dikshit et al. [62]. Meanwhile, this result is also consistent with the findings from Huang et al. [26] that the calcites crystals at pH of 8.0–9.0 are mainly in the spherical and square shapes, while crystals turn out to be amorphous-shape at pH around 7.0.

3.5. Effect of $CaCl_2$/urea loading rate

To optimize the $CaCl_2$/urea loading rate for the three stage biogrouting method, the molar concentration of $CaCl_2$ and urea were systematically studied with different $CaCl_2$ and urea concentration combinations. Firstly, three different $CaCl_2$ loading rate levels (0.25, 0.5 and 1.0 M) were studied by fixing the $CaCl_2$ to urea molar ratio at 1:1. With the increase of $CaCl_2$ daily loading rate from 0.25 to 0.5 M, the UCS increased from 1.4 to 7.3 MPa, while UCS dramatically drop down to 4.0 MPa when $CaCl_2$ concentration was further raised to 1.0 M (Table 4). This result could be because that ureolysis rate of *S. pasteurii-DSM 33-ASW100* was strongly inhibited under such high $CaCl_2$ level. As discussed in section 3.2, the alternative sites from urea were occupied by $CaCl_2$ so that urea cannot bind with urease anymore, resulting in the declining of hydrolysis rate and ultimately weakening the column strength. The low pH value (pH = 6.9) from the biocement solution also manifests that the hydrolysis of urea under high $CaCl_2$ level (1.0 M) was suppressed (Table 4). With the increase of $CaCl_2$ loading rate (0.25 to 0.5 M), the $CaCO_3$ content raised from 13.9 to 32.5 % and presented no significant increase as the $CaCl_2$ loading rate became over 0.5 M (Table 4). On the other hand, the calcium ion conversion efficiency from $CaCl_2$ to $CaCO_3$ was declining when $CaCl_2$ loading rate increases from 0.5 to 1.0 M (Table 4). One of the explanations is that the 32.5 % of $CaCO_3$ content was the saturated point for this particle size column, nearly 100 % of the void space had already been filled with $CaCO_3$ when $CaCl_2$ loading rate reached 0.5 M. Another reason could be that the MICP reaction under 1.0 M of $CaCl_2$ loading rate was incomplete and most of the calcium ions were still dissolved in the water without forming precipitation.

Table 4
Results of biogrouting performances and column properties for different combinations of urea and $CaCl_2$.

Urea (M)	$CaCl_2$ (M)	UCS (MPa)	Biocement solution pH	Ca^{2+} utilization efficiency (%)	$CaCO_3$ content (%)
0.25	0.25	1.4 ± 0.3	8.0 ± 0.7	23.3 ± 10.6	13.9 ± 5.4
0.50	0.50	7.3 ± 1.4	7.2 ± 0.6	82.4 ± 8.6	32.5 ± 2.4
1.00	1.00	4.0 ± 1.1	6.9 ± 0.8	46.2 ± 3.5	32.5 ± 1.9
1.00	0.50	9.1 ± 0.6	7.4 ± 0.2	85.2 ± 10.4	33.2 ± 3.4
2.00	0.50	2.6 ± 0.8	7.7 ± 0.5	63.4 ± 16.0	27.0 ± 5.2
4.00	0.50	2.0 ± 1.0	8.3 ± 0.2	68.5 ± 10.9	28.5 ± 2.9

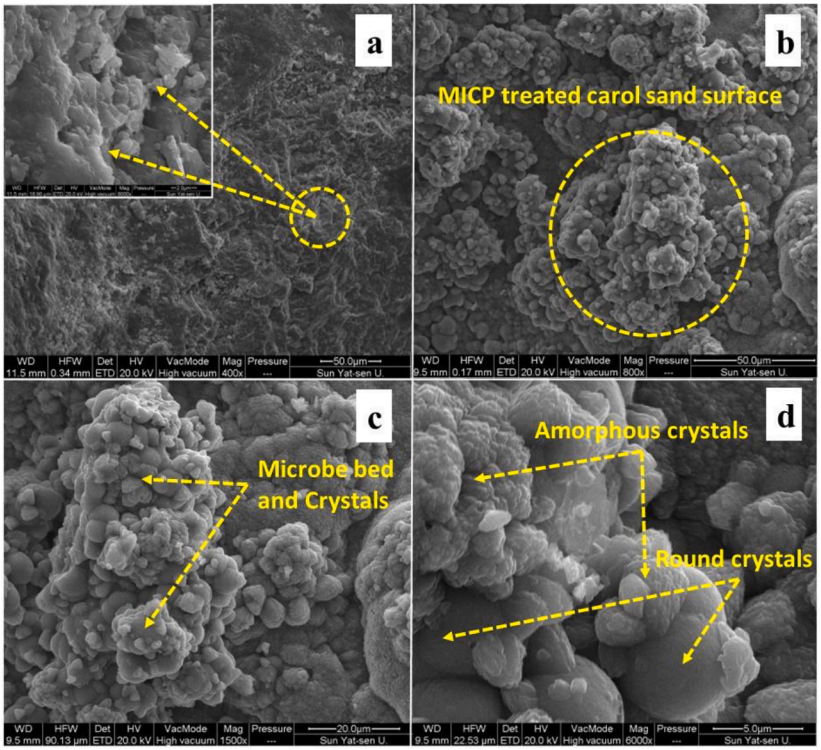

Fig. 8. SEM images of raw and MICP-treated coral sand via three-stage biogrouting method: (a) raw coral sand particles and a zoom-in view of the surface; (b) MICP-treated particle surface; (c) a zoom-in view of the microbe bed and crystals; (d) a zoom-in view of the crystal structure.

For the investigation of the effects of urea loading rate, the $CaCl_2$ loading rate 0.5 M was selected based on the results of UCS, $CaCO_3$ content and Ca^{2+} utilization efficiency. The urea concentration varied from 0.5 to 4.0 M. The pH results of the biocement solution were consistent with those of section 3.2 (Fig. 4c) that pH raised with the increase of urea loading rate (Table 4). However, the UCS kept increasing from 7.3 to 9.1 MPa when urea concentration raised from 0.5 to 1.0 M, while it dramatically dropped down to 2.0–2.6 MPa when further increasing the urea loading rate from 1.0 to 4.0 M (Table 4). Besides, it is noticeable that the two peaks of $CaCO_3$ content (~33 %) and Ca^{2+} utilization efficiency (~83 %) were achieved under lower urea loading rate conditions (0.5 and 1.0 M) (Table 4). It is possibly due to the fast ureolysis rate at high urea loading rate that a large amount of $CaCO_3$ precipitate is quickly formed and blocks the void space at the top layer while the lower layer or other void spaces are still empty without any biocement.

In addition, the fracture morphologies of the samples under different UCS strength levels, namely low (~1.4 MPa), medium (~4.0 MPa) and high (~9.1 MPa), provided extra evidence to the before-mentioned hypothesis (Fig. 9). For low strength columns (Fig. 9a I–III), lots of scattered coral sand particles fell off from the two boundary layers (top and bottom) of the column, due to incomplete crystallization and partial clogging inside the column body. On the other hand, for medium (Fig. 9b I–III) and high level (Fig. 9c I–III) strength column samples, less scattered coral sand particles were observed after the test. Moreover, most of the crack shapes from high level UCS strength (Fig. 9c II and III) presented an axe split pattern, namely splitting continuously from the top to the bottom layer of the entire column sample, which manifests the homogenous crystallization condition inside the column body.

The similar conclusion was also put forward in other studies that fast hydrolysis rate can easily produce large size but nonuniform calcite crystals, leading to reduced cell mobility in the column and non-homogeneous distribution [7,63–65]. Moreover, Lai et al. [66] and Liang et al. [67] even conducted the MICP process under low pH range (pH 3–6) to avoid excessive flocculation and clogging of the pore voids near the injection end. In addition, *S. pasteurii* from Zhao's lab can produce more urease when urea concentration increased from 0.08 to 0.25 M [47], uniform distribution of $CaCO_3$ precipitate was observed from Zhao's study though. This may because that the urease loading rate was far lower than this study. Thus, it can be concluded that high urea loading rate does improve the MICP activity, which however may lead to partial clogging phenomenon. Therefore, the moderate $CaCl_2$ (0.5 M) and urea (1.0 M) daily loading rate is recommended to avoid $CaCO_3$ crystallization distributing non-homogeneously within the column and thus to achieve high UCS. Similar conclusion was also provided by Lorena et al. [68] that the partial strength enhancement was no favor of improving MICP performance, the fineness of the cement was the factor that may influence the strength of the column.

4. Limitations and implications of current work

The present study approves the adaptability of the acclimated *S. pasteurii* to grow under high salinity environment without growth and urease secretion inhibition problem. In addition, the acclimated *S. pasteurii* can be obtained by conducting a long-term incubation under high salinity environment. The large-scale inoculation of *S. pasteurii* is feasible by the virtue of its high cell growth rate. Nonetheless, more cell growth test and MICP reaction performances should be evaluated under real seawater environment. In addition, the ability of *S. pasteurii* to compete with other species for nutrients utilization and to adapt to severe environments (such as pH, temperature, alkalinity etc.) should be also evaluated in field tests. Regarding to the costs, nitrogen and carbon sources such as casein peptone, soy peptone and urea for MICP in scale-up tests or real engineering practices would be more costly, comparing with traditional concrete. Therefore, to avoid over relying on industrial chemicals, vegetable-based proteins derived from agriculture waste such as soy protein isolate, corn gluten, dried distiller grain soluble, green bean and sweet potato skin could be selected as potential protein substrates to support cell growth for lower costs. Moreover, urea may also be collected from human daily urinate discharge or even from ocean.

The variation of pH with time under different urea and $CaCl_2$ concentrations and combinations provides the researchers some significant guidelines for future sandy desertification control, soil erosion control and even shoreline restoration by using MICP process. The maximum MICP reaction pH with the corresponding time consuming in section 3.2 was summarized into Table 5, which implicates that MICP reaction can be conducted under both alkaline and neutral pH environment by adjusting the molarity combination of calcium ion and urea. Thus, MICP process can be used to solidify sand from the top layer of the sand horizon or even reinforce the shoreline facility under a neutral pH condition without impacting the local soil or water ecological environment.

Regarding underwater applications, the MICP process can directly reinforce the coral sand in the seawater, which is more convenient and

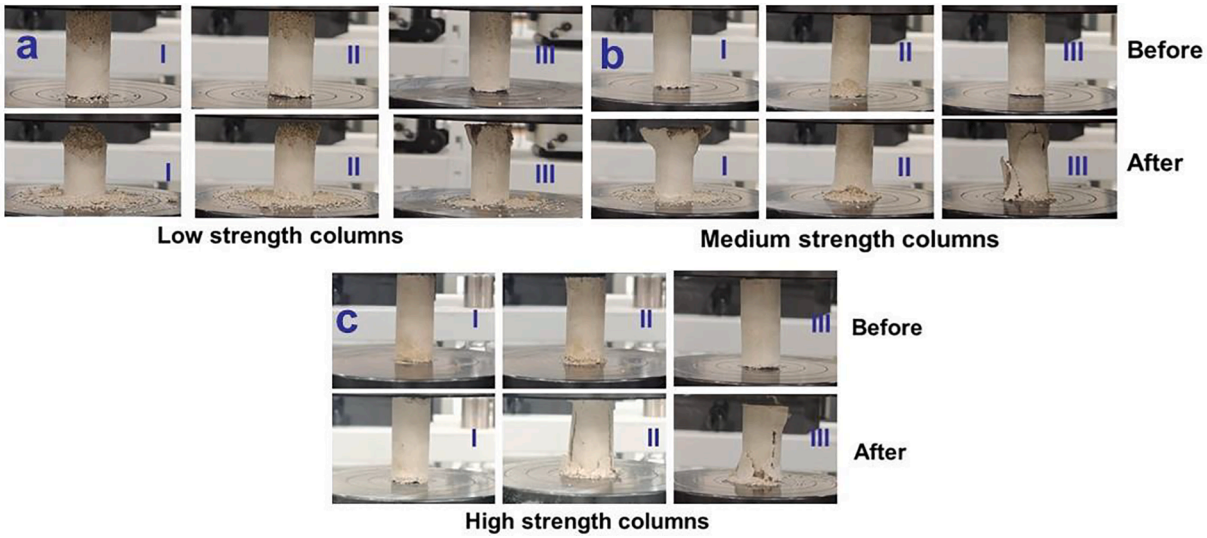

Fig. 9. The photos of different strength level column samples before and after the unconfined compressive test: (a) low strength columns, (b) mediums strength columns and (c) high strength column.

Table 5
The summarization of maximum pH with corresponding time consuming under different urea and $CaCl_2$ concentrations and treatments.

Treatments		Test results	
Urea (M)	$CaCl_2$ (M)	maximum pH	Time (min)
0.5	0.0	8.54 ± 0.02	180
0.5	0.25	8.47 ± 0.10	240
0.5	0.5	7.49 ± 0.01	300
0.5	1.0	6.75 ± 0.03	180
0.25	0.25	8.23 ± 0.03	300
0.5	0.25	8.47 ± 0.10	200
1.0	0.25	8.35 ± 0.10	120
0.5	0.5	7.49 ± 0.01	300
1.0	0.5	7.49 ± 0.03	300
2.0	0.5	7.70 ± 0.02	420
3.0	0.5	7.88 ± 0.02	360
4.0	0.5	8.40 ± 0.09	420
0.5	1.0	6.75 ± 0.03	240
1.0	1.0	6.95 ± 0.06	240
2.0	1.0	7.18 ± 0.07	300
3.0	1.0	7.17 ± 0.05	360
4.0	1.0	7.30 ± 0.10	420
6.0	1.0	7.59 ± 0.09	300
8.0	1.0	8.06 ± 0.17	320

less expensive than the traditional concrete solidification process. Moreover, cells are easier to transport into the voids of sand and form more uniform biocement. For the economic aspects, the ocean can provide abundant of $CaCl_2$ to support the MICP reaction, which can greatly decrease the chemical cost. As to the safety concern of marine ecological environment, MICP process is natural microbial activity, which is less harmful to marine organism comparing with traditional concrete. However, the pumping and biogrouting system in the present study may not be directly applicable to the reinforcement of coral sand in the deep ocean. In future, engineering practice can be conducted with the following concerns: 1) special pipe and pumping system should be systematically designed to sustain high pressure in the deep ocean environment and 2) the establishment of an enclosed workspace under the water environment can improve the MICP process efficiency and avoid negative influence of other marine organisms to *S. pasteurii*.

5. Conclusion

In this study, a new *Sporosarcina pasteurii* strain, *S. pasteurii-DSM 33-ASW100*, was acclimated under seawater environment. The mechanism of potential calcium chloride inhibition to *S. pasteurii-DSM 33-ASW100* was investigated, and potential solution to overcome this inhibition phenomenon was proposed. In the biogrouting test, the coral sand particle size optimization test was firstly investigated. Then, an improved three-stage biogrouting method was developed based on the traditional two-stage biogrouting method. Finally, based on the three-stage biogrouting method, an optimization test was conducted under a variety of urea/$CaCl_2$ concentrations. Several concluding remarks were drawn as below.

1) *S. pasteurii* can adapt to the growth environment under different salinity conditions, and long-term growth in high-salinity seawater environment was more conducive to the growth of cells as well as the ureolysis activity.
2) High concentration of calcium chloride (>0.25 M) inhibited urease activity, but hardly affected the physiological characteristics of *S. pasteurii-DSM 33-ASW100*. Increasing the dosage of urea cannot alleviate the inhibitory effect of calcium chloride on urease activity, but it can stimulate *S. pasteurii-DSM 33-ASW100* to produce more renascent urease.
3) The particle size of coral sand optimal for biocementation is around 0.5–1.0 mm. The proposed three-stage grouting method can mitigate the issue of non-uniform distribution of cells and crystals in the column, thereby greatly increasing the strength of MICP-treated samples.
4) Increasing the dosage of calcium chloride can increase the strength of the column to a certain extent, but excessive input of calcium ions may result in less uniformity of crystallization and thus lead to a relative lower USC. Excessive addition of urea increased the ureolysis rate, while this may lead to partial clogging issues due to too fast reaction of MICP.

Declaration of Competing Interest

The authors declare that they have no known competing financial interests or personal relationships that could have appeared to influence the work reported in this paper.

Data availability

Data will be made available on request.

Acknowledgments

This work has been financially supported by the National Natural Science Foundation of China (51909289, 51978677, 52111530089), the Shenzhen Science and Technology Project for Sustainable Development (KCXFZ202002011008532), and the Shenzhen Natural Science Foundation (JCYJ20190807399162401662).

References

[1] L. Liu, H. Liu, Y. Xiao, J. Chu, P. Xiao, Y. Wang, Biocementation of calcareous sand using soluble calcium derived from calcareous sand, Bulletin of Engineering Geology and the Environment 77 (2018) 1781–1791.
[2] M. Coop, The mechanics of uncemented carbonate sands, Géotechnique 40 (1990) 607–626.
[3] D. Terzis, L. Laloui, A decade of progress and turning points in the understanding of bio-improved soils: A review, Geomechanics for Energy and the Environment 19 (2019), 100116.
[4] L. Cheng, M. Shahin, R. Cord-Ruwisch, M. Addis, T. Hartanto, C. Elms, Soil stabilisation by microbial-induced calcite precipitation (MICP): investigation into some physical and environmental aspects, 7th international congress on environmental geotechnics, Australia, Engineers Australia Melbourne, 2014, pp. 1105–1112.
[5] Y.J. Phua, A. Røyne, Bio-cementation through controlled dissolution and recrystallization of calcium carbonate, Construction and Building Materials 167 (2018) 657–668.
[6] V. Ivanov, J. Chu, Applications of microorganisms to geotechnical engineering for bioclogging and biocementation of soil in situ, Reviews in Environmental Science and Bio/Technology 7 (2008) 139–153.
[7] W. De Muynck, N. De Belie, W. Verstraete, Microbial carbonate precipitation in construction materials: a review, Ecological engineering 36 (2010) 118–136.
[8] M.S. Reddy, S. Joshi, Carbon dioxide sequestration on biocement-based composites, Carbon dioxide sequestration in cementitious construction materials (2018) 225–243.
[9] R. Abdel-Basset, E.A. Hassan, H.-P. Grossart, Manifestations and environmental implications of microbially-induced calcium carbonate precipitation (MICP) by the cyanobacterium Dolichospermum flosaquae, Biogeosciences Discussions (2020) 1–20.
[10] D. Ariyanti, N. Handayani, Hadiyanto (2012) Feasibility of using microalgae for biocement production through biocementation, J Bioprocess Biotechniq 2 (2012) 2.
[11] A.F. Alshalif, J. Irwan, N. Othman, L. Anneza, Isolation of sulphate reduction bacteria (SRB) to improve compress strength and water penetration of bio-concrete, MATEC Web of Conferences, EDP Sciences (2016) 01016.
[12] F.M. Lapierre, J. Schmid, B. Ederer, N. Ihling, J. Büchs, R. Huber, Revealing nutritional requirements of MICP-relevant Sporosarcina pasteurii DSM33 for growth improvement in chemically defined and complex media, Scientific Reports 10 (2020) 1–14.
[13] A.I. Omoregie, L.H. Ngu, D.E.L. Ong, P.M. Nissom, Low-cost cultivation of Sporosarcina pasteurii strain in food-grade yeast extract medium for microbially induced carbonate precipitation (MICP) application, Biocatalysis and Agricultural, Biotechnology 17 (2019) 247–255.
[14] P. Liu, G.-H. Shao, R.-P. Huang, Study of the interactions between S. pasteurii and indigenous bacteria and the effect of these interactions on the MICP, Arabian Journal of Geosciences 12 (2019) 1–10.
[15] L. Chen, Y. Song, H. Fang, Q. Feng, C. Lai, X. Song, Systematic optimization of a novel, cost-effective fermentation medium of Sporosarcina pasteurii for

microbially induced calcite precipitation (MICP), Construction and Building Materials 348 (2022), 128632.
[16] F.M. Lapierre, J. Schmid, B. Ederer, N. Ihling, J. Büchs, R. Huber, Publisher Correction: Revealing nutritional requirements of MICP-relevant Sporosarcina pasteurii DSM33 for growth improvement in chemically defined and complex media, Scientific Reports 12 (2022) 1–3.
[17] C.-S. Tang, L.-Y. Yin, N.-J. Jiang, C. Zhu, H. Zeng, H. Li, B. Shi, Factors affecting the performance of microbial-induced carbonate precipitation (MICP) treated soil: a review, Environmental Earth Sciences 79 (2020) 1–23.
[18] J. Intarasoontron, W. Pungrasmi, P. Nuaklong, P. Jongvivatsakul, S. Likitlersuang, Comparing performances of MICP bacterial vegetative cell and microencapsulated bacterial spore methods on concrete crack healing, Construction and Building Materials 302 (2021), 124227.
[19] A.A. Nasser, N.M. Sorour, M.A. Saafan, R.N. Abbas, Microbially-Induced-Calcite-Precipitation (MICP): A biotechnological approach to enhance the durability of concrete using Bacillus pasteurii and Bacillus sphaericus, Heliyon 8 (2022) e09879.
[20] M.G. Sohail, Z. Al Disi, N. Zouari, N. Al Nuaimi, R. Kahraman, B. Gencturk, D. F. Rodrigues, Y. Yildirim, Bio self-healing concrete using MICP by an indigenous Bacillus cereus strain isolated from Qatari soil, Construction and Building Materials 328 (2022), 126943.
[21] D. Sarda, H.S. Choonia, D. Sarode, S. Lele, Biocalcification by Bacillus pasteurii urease: a novel application, Journal of Industrial Microbiology and Biotechnology 36 (2009) 1111–1115.
[22] S. Al-Thawadi, R. Cord-Ruwisch, Calcium carbonate crystals formation by ureolytic bacteria isolated from Australian soil and sludge, J. Adv. Sci. Eng. Res 2 (2012) 12–26.
[23] L. Cheng, C. Qian, R. Wang, J. Wang, Study on the mechanism of calcium carbonate formation induced by carbonate-mineralization microbe, Acta Chimica Sinica 65 (2007) 2133–2138.
[24] R. Wang, C. Qian, J. Wang, Study on microbiological precipitation of CaCO3, Journal of Southeast University (Natural Science Edition) 35 (2005) 191–195.
[25] S. Stocks-Fischer, J.K. Galinat, S.S. Bang, Microbiological precipitation of CaCO3, Soil Biology and Biochemistry 31 (1999) 1563–1571.
[26] Y. Huang, X.-G. Luo, F. Du, Studies on the effect factor of microbiologically induced calcite precipitation, Journal of Southwest University of, Science and Technology 24 (2009) 87–93.
[27] C.M. Gorospe, S.-H. Han, S.-G. Kim, J.-Y. Park, C.-H. Kang, J.-H. Jeong, J.-S. So, Effects of different calcium salts on calcium carbonate crystal formation by Sporosarcina pasteurii KCTC 3558, Biotechnology and bioprocess engineering 18 (2013) 903–908.
[28] Y. Zhang, H. Guo, X. Cheng, Influences of calcium sources on microbially induced carbonate precipitation in porous media, Materials Research Innovations, 18 (2014) S2-79-S72-84.
[29] V.S. Whiffin, L.A. Van Paassen, M.P. Harkes, Microbial carbonate precipitation as a soil improvement technique, Geomicrobiology Journal 24 (2007) 417–423.
[30] M. Cui, J. Zheng, H. Lai, Effect of method of biological injection on dynamic behavior for bio-cemented sand, Rock and Soil Mechanics 38 (2017) 3173–3178.
[31] V. Rebata-Landa, Microbial activity in sediments: effects on soil behavior, Georgia Institute of Technology (2007).
[32] M.S. Ashraf, S.B. Azahar, N.Z. Yusof, Soil improvement using MICP and biopolymers: A review, IOP Conference Series: Materials Science and Engineering, IOP Publishing (2017), 012058.
[33] L. Van Paassen, M. Harkes, G. Van Zwieten, W. Van der Zon, W. Van der Star, M. Van Loosdrecht, in: Scale up of BioGrout: a Biological Ground Reinforcement Method, IOS Press, 2009, pp. 2328–2333.
[34] B. Li, Geotechnical properties of biocement treated soils, Nanyang Technological University, PhD diss., 2014.
[35] A.A. Qabany, K. Soga, Effect of chemical treatment used in MICP on engineering properties of cemented soils, Bio-and Chemo-Mechanical Processes in Geotechnical Engineering: Géotechnique Symposium in Print, ICE Publishing 2014 (2013) 107–115.
[36] F. Kunst, G. Rapoport, Salt stress is an environmental signal affecting degradative enzyme synthesis in Bacillus subtilis, Journal of bacteriology 177 (1995) 2403–2407.
[37] W. Deng, Y. Wang, Investigating the factors affecting the properties of coral sand treated with microbially induced calcite precipitation, Advances in civil Engineering 2018 (2018).
[38] A. Mahawish, A. Bouazza, W.P. Gates, Strengthening crushed coarse aggregates using bio-grouting, Geomechanics and Geoengineering 14 (2019) 59–70.
[39] Z.B. Bundur, A. Amiri, Y.C. Ersan, N. Boon, N. De Belie, Impact of air entraining admixtures on biogenic calcium carbonate precipitation and bacterial viability, Cement and Concrete Research 98 (2017) 44–49.
[40] A. Martinez, L. Huang, M. Gomez, Thermal conductivity of MICP-treated sands at varying degrees of saturation, Géotechnique Letters 9 (2019) 15–21.
[41] Z. Gu, X. Li, J. Wu, S. Niu, P. Wang, D. Yao, J.-J. Zheng, J. Yan, L. Xu, M. Yang, A Novel Strategy for Reinforcing Cementation Process Coupling Microbially Induced Carbonate Precipitation (Micp) with Cross-Linked Silk Fibroin, Available at SSRN 4065692.
[42] C. Konstantinou, Y. Wang, G. Biscontin, K. Soga, The role of bacterial urease activity on the uniformity of carbonate precipitation profiles of bio-treated coarse sand specimens, Scientific reports 11 (2021) 1–17.
[43] L. Cheng, R. Cord-Ruwisch, M.A. Shahin, Cementation of sand soil by microbially induced calcite precipitation at various degrees of saturation, Canadian Geotechnical Journal 50 (2013) 81–90.
[44] R. Xiao, X. Li, Y. Zheng, Comprehensive study of cultivation conditions and methods on lipid accumulation of a marine protist, Thraustochytrium striatum, Protist 169 (2018) 451–465.
[45] Q. Fu, Y. Wu, S. Liu, L. Lu, J. Wang, The adaptability of Sporosarcina pasteurii in marine environments and the feasibility of its application in mortar crack repair, Construction and Building Materials 332 (2022), 127371.
[46] S. Svane, J.J. Sigurdarson, F. Finkenwirth, T. Eitinger, H. Karring, Inhibition of urease activity by different compounds provides insight into the modulation and association of bacterial nickel import and ureolysis, Scientific reports 10 (2020) 1–14.
[47] Q. Zhao, L. Li, C. Li, M. Li, F. Amini, H. Zhang, Factors affecting improvement of engineering properties of MICP-treated soil catalyzed by bacteria and urease, Journal of Materials in Civil Engineering 26 (2014) 04014094.
[48] J.P. Carmona, P.J.V. Oliveira, L.J. Lemos, Biostabilization of a sandy soil using enzymatic calcium carbonate precipitation, Procedia engineering 143 (2016) 1301–1308.
[49] S.P. Chaparro-Acuña, M.L. Becerra-Jiménez, J.J. Martínez-Zambrano, H.A. Rojas-Sarmiento, Soil bacteria that precipitate calcium carbonate: mechanism and applications of the process, Acta Agronómica 67 (2018) 277–288.
[50] R. Xiao, X. Li, Y. Zheng, Enzyme production by a fungoid marine protist, Thraustochytrium striatum, European journal of protistology 66 (2018) 136–148.
[51] D. Terzis, L. Laloui, 3-D micro-architecture and mechanical response of soil cemented via microbial-induced calcite precipitation, Scientific reports 8 (2018) 1–11.
[52] K. Kirsch, F. Kirsch, Ground improvement by deep vibratory methods, Taylor & Francis, 2017.
[53] D. Guangyin, G. Changhui, L. Songyu, P. Huangsong, G. Qian, L. Tao, Resonance vibration approach in soil densification: laboratory experiences and numerical simulation, Earthquake Engineering and Engineering Vibration 20 (2021) 317–328.
[54] D. Xu, Z. Zhang, Y. Qin, Y. Yang, Effect of particle size on the failure behavior of cemented coral sand under impact loading, Soil Dynamics and Earthquake Engineering 149 (2021), 106884.
[55] X. Fang, Y. Yang, Z. Chen, H. Liu, Y. Xiao, C. Shen, Influence of fiber content and length on engineering properties of MICP-treated coral sand, Geomicrobiology Journal 37 (2020) 582–594.
[56] S. Alghamdi, F. Du, J. Yang, G. Pinder, T. Tan, Tensile and shear behavior of microscale growth layers between nacre in red abalone, Journal of the Mechanics and Physics of Solids 138 (2020), 103928.
[57] G. Falini, G. Sartor, D. Fabbri, P. Vergni, S. Fermani, A.M. Belcher, G.D. Stucky, D. E. Morse, The interstitial crystal-nucleating sheet in molluscan Haliotis rufescens shell: a bio-polymeric composite, Journal of structural biology 173 (2011) 128–137.
[58] B.L. Smith, T.E. Schäffer, M. Viani, J.B. Thompson, N.A. Frederick, J. Kindt, A. Belcher, G.D. Stucky, D.E. Morse, P.K. Hansma, Molecular mechanistic origin of the toughness of natural adhesives, fibres and composites, Nature 399 (1999) 761–763.
[59] M.A. Meyers, A.-Y.-M. Lin, P.-Y. Chen, J. Muyco, Mechanical strength of abalone nacre: role of the soft organic layer, Journal of the mechanical behavior of biomedical materials 1 (2008) 76–85.
[60] Z.-J. Zhang, K.-W. Tong, L. Hu, Q. Yu, L.-L. Wu, Experimental study on solidification of tailings by MICP under the regulation of organic matrix, Construction and Building Materials 265 (2020), 120303.
[61] T. Ghosh, S. Bhaduri, C. Montemagno, A. Kumar, Sporosarcina pasteurii can form nanoscale calcium carbonate crystals on cell surface, PLoS One 14 (2019) e0210339.
[62] R. Dikshit, A. Dey, A. Kumar, Sporosarcina pasteurii can Efficiently Precipitate Calcium Carbonate at High Salt Concentration, Geomicrobiology Journal 39 (2022) 123–134.
[63] B. Mortensen, J. DeJong, Strength and stiffness of MICP treated sand subjected to various stress paths, Geo-Frontiers, Advances in Geotechnical Engineering 2011 (2011) 4012–4020.
[64] K. Rowshanbakht, M. Khamehchiyan, R.H. Sajedi, M.R. Nikudel, Effect of injected bacterial suspension volume and relative density on carbonate precipitation resulting from microbial treatment, Ecological Engineering 89 (2016) 49–55.
[65] J. Gleaton, Z. Lai, R. Xiao, K. Zhang, Q. Chen, Y. Zheng, Optimization of mechanical strength of biocemented Martian regolith simulant soil columns, Construction and Building Materials 315 (2022), 125741.
[66] Y. Lai, J. Yu, S. Liu, J. Liu, R. Wang, B. Dong, Experimental study to improve the mechanical properties of iron tailings sand by using MICP at low pH, Construction and Building Materials 273 (2021), 121729.
[67] L. Cheng, M.A. Shahin, J. Chu, Soil bio-cementation using a new one-phase low-pH injection method, Acta Geotechnica 14 (2019) 615–626.
[68] L. Skevi, B.J. Reeksting, T.D. Hoffmann, S. Gebhard, K. Paine, Incorporation of bacteria in concrete: The case against MICP as a means for strength improvement, Cement and Concrete Composites 120 (2021), 104056.